**INDONESIAN JOURNAL OF GEOGRAPHY**

# Assessing the Potential of LAPAN-A3 Data for Landuse/landcover Mapping

**Zylshal Zylshal, Rahmad Wirawan and Dony Kushardono**

**Abstract** LAPAN-A3/LAPAN-IPB is the third generation of micro-satellite developed by Indonesian National Institute of Aeronautics and Space (LAPAN). The satellite carries a multispectral push-broom sensor that can record the earth's surface at the visible and near-infrared spectrum. Being launched in June 2016, there has no been many publications related to the use of LAPAN-A3 multispectral data for landuse/landcover (LULC) mapping. This paper aims to provide information regarding the use of LAPAN-A3 data for the LULC extraction using a maximum likelihood algorithm as well as the artificial neural network and then evaluate the results. The LAPAN-A3 image was geometrically corrected by using Landsat-8 OLI image as reference data. Three test areas with a size of 1200x945 pixels are then selected for pixel-based classification with the two algorithms mentioned above. For comparison, both LAPAN-A3 and Landsat-8 data were classified for 3 test areas. Accuracy assessment was performed on both datasets using manually interpreted SPOT-6 Pansharpened image as reference data. Preliminary results showed that LAPAN-A3 were able to extract  ten-different LULC classes, comprises of built-up area, forest, rivers, fishponds, shrubs, wetland forests, rice fields, sea, agricultural land, and bare soil. The overall accuracy of LAPAN-A3 data is generally lower than Landsat-8, which ranges from 49.76% to 71.74%. These results illustrate the potential of LAPAN-A3 data to derive LULC information. The lack of necessary parameters to perform radiometric correction and blurring effect are several issues that need to be solved to improve the accuracy LULC.

**Keywords:** LAPAN-A3, Landsat-8, LULC, Maximum Likelihood, Neural Network

**Abstrak** *LAPAN-A3/LAPAN-IPB adalah mikrosatelit generasi ketiga yang dikembangkan oleh Lembaga Penerbangan dan Antariksa Nasional (LAPAN). Satelit ini membawa muatan berupa sensor pushbroom multispektral yang dapat merekam permukaan bumi pada panjang gelombang tampak dan inframerah dekat. Diluncurkan pada Bulan Juni 2016, sampai saat ini, publikasi terkait dengan penggunaan data multispektral LAPAN-A3 untuk pemetaan penutup/penggunaan lahan masih terbatas. Tulisan ini bertujuan untuk memberikan informasi terkait penggunaan data LAPAN-A3 untuk ekstraksi informasi penutup penggunaan lahan dengan menggunakan algoritma maximum likelihood dan artificial neural network lalu mengevaluasi hasilnya. Citra LAPAN-A3 dikoreksi geometrik dengan menggunakan citra Landsat-8 OLI sebagai data referensi. Tiga test area dengan ukuran 1200x945 piksel kemudian dipilih untuk dilakukan klasikasi berbasis piksel dengan algoritma maximum likelihood. Untuk perbandingan, baik data LAPAN-A3 dan Landsat-8 masing-masing diklasifikasi untuk 3 test area. Uji akurasi dilakukan untuk kedua data dengan menggunakan citra SPOT-6 Pansharpened sebagai data referensi. Hasil awal menunjukkan bahwa kelas penutup/penggunaan lahan yang bisa diekstrak secara digital dari LA-PAN-A3 antara lain adalah kelas lahan terbangun, hutan lahan kering, sungai, tambak, semak belukar, hutan lahan basah, sawah, laut, ladang, dan lahan terbuka. Overall accuracy data LAPAN-A3 umumnya lebih rendah dari Landsat-8, yang berkisar antara 49.76% sampai 71.74%.  Masih belum sempurnanya kualitas radiometrik pada LAPAN-A3 dan blurring effect menjadi isu yang perlu diselesaikan untuk meningkatkan akurasi ekstraksi penutup/penggunaan lahan secara digital.*

*Kata kunci: LAPAN-A3, Landsat-8, Penutup/penggunaan lahan, Maximum Likelihood, Neural Network*

## 1.Introduction

The LAPAN-A3/LAPAN-IPB satellite was successfully launched in June 2016 from Satihs Dhawan Space Center, Sriharikota, India. It carries a multispectral push-broom scanner, dubbed as Land Imager Space Application (LISA), with 15-meter spatial resolution, among other payloads. The multispectral sensor has four bands ranging from visible to near infrared spectrum. With the swath width of 123 km, LISA's spectral data can be categorized as medium resolution Earth Observation (EO) data.

Until recently, most of the publication on LAPAN-A3 were about the satellite technology itself (Hakim, Hasbi, & Syafrudin, 2014; Hasbi & Suhermanto, 2013) and data compresion (Hakim & Permala, 2017). Very few studies have been done on LAPAN-A3 LISA data utilization. Zylshal et al. (2017) reported that LAPAN-A3 has radiometric problems, and despite having this problem, it still managed to get a moderate correlation especially in NIR and Red spectrum with Sentinel-2 MSI. Considering how useful both of these band on generating vegetation indices (Du et al., 2016; Han, Wu, Tahmassebi, Xu, & Wang, 2011; McFeeters, 1996) and on biophysical parameter extraction (Knipling,

**Zylshal and Dony Kushardono**
Remote Sensing Applications Center, Indonesian National Institute of Aeronautics and Space (LAPAN)

**Rahmad Wirawan**
Department of Geography, Faculty of Social Science, Universitas Negeri Malang

Correspondent e-mail:zylshal@lapan.go.id

1970; Tucker & Sellers, 1986; Veraverbeke et al., 2012; Yoshioka, Huete, & Miura, 2000), it is important to see its potentiality on deriving landuse/landcover information. Setiawan et al. (2018) evaluate LAPAN-A3 spectral features to identify agricultural landuse types in Java and found adequate spectral discrimination of crop types. Nugroho, Zylshal, & Kushardono (2018) conducted a more generalized LULC extraction from LAPAN-A3 over some part of Danau Toba, in North Sumatra, Indonesia, and found a high overall accuracy, albeit for only five landcover classes and a small sample size. A careful examination of their study area shows a large portion of the water body and forest. How it performs on a more complex LULC in a different area with different characteristics remains to be explored.

Landuse/landcover (LULC) plays a critical role in understanding the functioning of terrestrial ecosystem in terms of biogeochemical cycling, hydrological processes, and the interaction between the surface and the atmosphere (Wahid & Akiyama, 2007). This paper aims to evaluate LAPAN-A3 potential on extracting up-to-date LULC map. One of the LAPAN-A3 main mission is for resource monitoring. LULC information is the basis of monitoring environment.

## 2. The Methods

The LAPAN-A3 image used in this study was acquired on October 19th, 2016 with relatively minimum cloud cover compared to the other scene acquired by LAPAN-A3 at the time. The characteristics of LAPAN-A3 data compared to Landsat-8 are represented in Table 1. As the data itself was still in the early stage, the necessary information required for atmospheric correction has not been available. Thus, this study used digital number (DN) value for both datasets in further analysis. Having analyzed imagery with different radiometric resolution (Table 1), LAPAN-A3 sensors have a few flaws which must be overcome before it can be used for operational purposes. The initial study conducted by Zylshal et al. (2017) found an uneven illumination across the LAPAN-A3 entire scene. Misalignment on each individual band is also apparent on LAPAN-A3 data (Hakim, Syafrudin, & Utama, 2017; Tahir et al., 2016). This then results in blurriness when RGB composite was made. Further details regarding this issue and a workaround for it is discussed later in this article.

Before conducting the landuse/landcover classification, both of the datasets undergone a preprocessing step. While Hakim et al. (2017) proposed a band co-registration method to minimize the misalignment with the final results lies within 1-3 pixel error, we decided to deploy a different approach method to have a subpixel accuracy. First, the geometric correction was done to the LAPAN-A3 using Landsat-8 orthorectified data as the reference. Geometric correction performed using image-to-

Table 1. Characteristics of LAPAN-A3 compared to Landsat-8

| Satellite | Sensor | Band | Spectral Range | Spatial Resolution | Swath Width | Revisit time | Radiometric Quantization |
|---|---|---|---|---|---|---|---|
| LAPAN-A3 | LISA - Line Imager Space Aplication | B1 - Blue B2 - Green B3 - Red B4 - NIR | 0.41 – 0.49 μm 0.51 – 0.58 μm 0.63 – 0.70 μm 0.77 – 0.99 μm | 15 m 15 m 15 m 15 m | 122,4 km | 21 days | 16bit |
| Landsat-8 | OLI (Operational Land Imager) | B1 - Coastal Aerosol B2 - Blue B3 - Green B4 - Red B5 - NIR B6 - SWIR 1 B7 - SWIR 2 | 0.43 – 0.45 μm 0.45 – 0.51 μm 0.53 – 0.59 μm 0.64 – 0.67 μm 0.85 – 0.88 μm 1.57 – 1.65 μm 2.11 – 2.29 μm | 30 m 30 m 30 m 30 m 30 m 30 m | 185 km | 16 days | 12bit |

Source: (PUSTEKSAT, 2016; USGS, 2012)

image registration method (Danoedoro, 2012; Jensen, 2005) with a minimum of 50 ground control points (GCP) used. In this study, the geometric correction was conducted for each pair of the band from both datasets, with the root mean square error (RMSE) maintained at less than 0.5 pixels. This degree of RMSE deemed acceptable for the geometric correction (Dai, 1998; Jensen, 2005). At this point, image co-registration involved resampling procedure that often reduced the image quality (Parker, Kenyon, & Troxel, 1983). To overcome this, we decided to use nearest neighbor algorithm to perform the resampling procedure. Li et al. (2013) found that nearest neighbor is able to maintain the pixel's original gray level relative to other interpolation methods (i.e., cubic convolution and bilinear). LAPAN-A3 data was resampled to 30 meters following Landsat-8 pixel size.  Figure 1 shows the two datasets used in this study. Unfortunately, the two scenes did not fully cover each other. With a larger swath width, Landsat-8 data only cover about 60% of LAPAN-A3 (figure 1). Considering these circumstances, we created three test sites on both datasets to be further analyzed.

These test sites were placed relatively close to the central region of the LAPAN-A3 entire scene with the size of 1200 x 945 pixel. Test site #1 (AOI_1) is located in Besuki Region, East Java. AOI_1 comprise of mixed forest and barren land on a hilly region, as well as agricultural land on a relatively flat coastal area. Test site #2 (AOI_2) located in Bondowoso Region, East Java. AOI_2 located in valley region between two volcanic mountain, Mt. Raung in the east and Mt. Argapura in the west. It mostly consists of mixed agriculture and mixed forest on slope area, albeit not as steep as the hilly region in AOI_1. Test site #3 (AOI_3) located in Jember Region, East Java is a much bigger city than the other two test sites. Thus, comprised of much more built-up features. AOI_3 has similar terrain as AOI_2.

Since both datasets differ in term of spectral resolution, this study only used 4 bands on Landsat-8 instead of the full band. Only blue, green, red, and near-infrared bands were used in the further process. Two classification algorithms were employed to extract the LULC information from both sensors. First, one of the widely adopted parametric classification called maximum likelihood classifier (MLC) (Bailly, Arnaud, & Puech, 2007; Kanellopoulos, Wilkinson, & Megier, 1993; Liu, Skidmore, & Van Oosten, 2002). The algorithm is based on the assumption that radiometric values for each class are normally distributed. More details of the MLC can be found in (Richards, 1993; Schowengerdt, 1983). The second algorithm was the non-parametric classification called artificial neural network classifier (ANN). This algorithm is a popular learning method (Liu et al., 2002) and has been incorporated in many digital image processing

Table 2. Landuse/landcover classification system

| LULC | Description |
| --- | --- |
| Built-up | Including settlements, industrial complexes, and other built-up feature |
| Forest | Tree height is more than 2 meters, whether it is ever-green or deciduous, broadleaf,  natural or artificial |
| River | Natural inland waterbody with an elongated shape |
| Fishpond | Inland man-made waterbody in the coastal region for fish or shrimp. Filled with brackish water, with distinct dike pattern |
| Shrubs | Dryland areas with various heterogeneous natural vegetation. Vegetation density varies from sparse to dense. Dominated by low vegetation (50 cm – 2 m) |
| Wetland Forest | Lowland wetland forest stretched along the coast of a low-altitude area and still affected by tides. |
| Ricefield | An irrigated-flooded field where rice crops are grown |
| Sea | Coastal waterbody including the sea, coral reefs, and seagrass. |
| Baresoil | Open land with vegetation canopy cover is less than 5%. Occur naturally and usually consisted of rock, stones or gravel, sand, soil, etc. |
| Other Agricultural | Seasonal plants other than rice grown in wetlands. Agricultural land prepared for planting by flooding the soil for a certain period of time |

Source: BSN (2014)

software (Harris® ENVI, PCI® Geomatics, ERDAS-Imagine, ORFEO Toolbox, etc.). Detailed explanation on ANN can be found in (Richards, 1993; Rumelhart, Hinton, & Williams, 1986). In this study, we used ENVI® 4.8 to deploy both classification algorithm.

Referring to the well established Indonesian national standard for landcover classification (BSN, 2014), this study utilizes landuse/landcover classes for 1:250.000. As the document itself is intended for visual interpretation, only a few selected classes were chosen to be utilized. Ten landuse/landcover classes were identified based on visual interpretation of Landsat-8 data, verified by the SPOT-6 panchromatic image. Table 2 shows the landuse/landcover classification ystem used in this study.

Following the preprocessing stage, both datasets were classified using two aforementioned classification algorithm with the same training area. While the training area was identical, each statistics for both datasets were calculated separately. In this study, we used the multi-layer perceptron trained by the back-propagation neural network algorithm (Rumelhart et al., 1986), employed within ENVI® Software package.

Our ANN classification parameters was chosen based on previous studies conducted by (G. M. Foody & Arora, 1997). Based on Kushardono et al. (1995), the optimum results for ANN can be achieved when the numbers of hidden layers kept at minimumum, with hidden neuron layer twice the amount of classes being

investigated. The training rate and training momentum should be on the opposite spectrum. If the training rate is set on high value (i.e 0.9), then the training momentum should be set on low value (i.e 0.1), and vice versa. (G. M. Foody & Arora, 1997) further agreed with previous founding and stating that increasing the size and complexity of the network will incur extra computational and ground data cost, with only a slight increase on classification accuracy. The more hidden layers being used, the more interaction between neurons and in between layers, where the process of finding the offset and gain value of each neuron is more complicated (Kushardono et al., 1995). We, therefore, decided to use only a single hidden layer to optimize computational time and classification accuracy. The ANN's number of training Iteration were set at 50000, with the RMS exit criteria of 0.005. With this value, the ANN training will stop should it reached one of the aforementioned criteria. This means that, the training did not neccesary reach 50000 iteration to finished. If the RMS exit criteria of 0.005, the training will stop. The complete parameters, based on our experimental results are shown in table 3.

The Accuracy assessment was done using confusion matrix (Congalton & Green, 2009). Cogen's kappa (κ) (Cohen, 1960) was also calculated. It is important to have the reference image as close as possible to the LAPAN-A3 acquisition date. Unfortunately, due to excessive cloud coverage in the area, the closest and
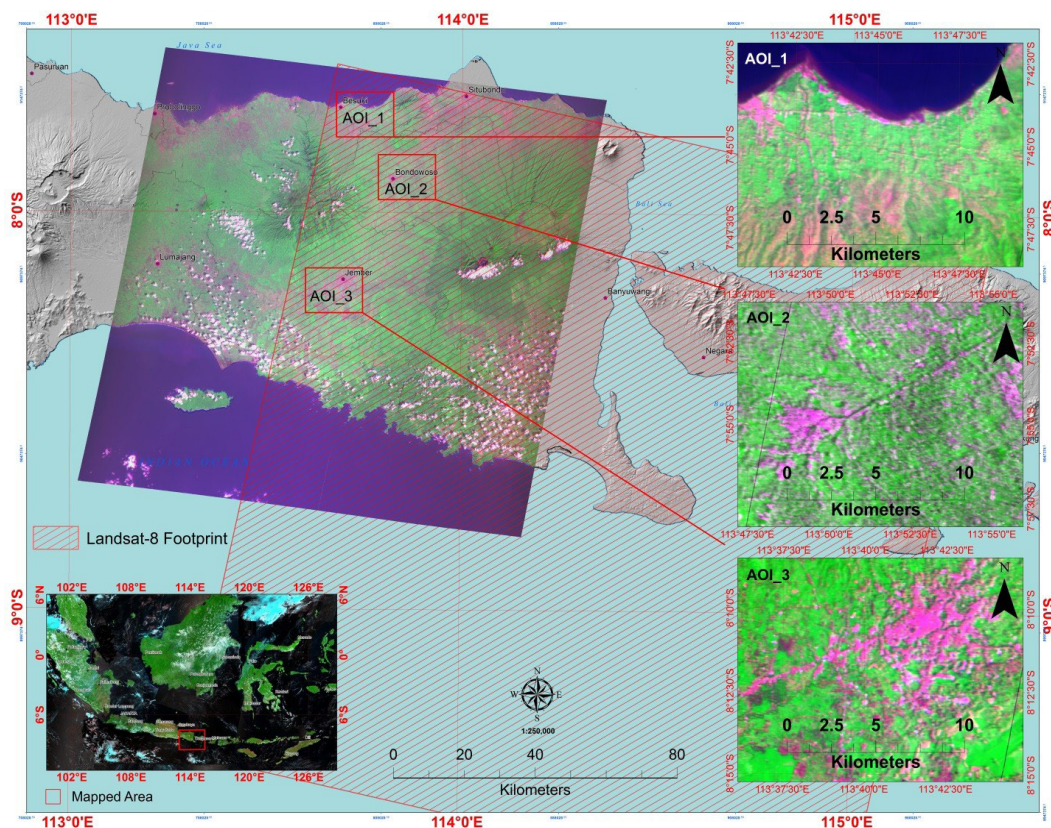


Figure 1. Study area. LAPAN-A3 entire scene shown as RGB (Red-NIR-Green), with Landsat-8 footprint over-layed on top as gradient-line-filled rectangle. Three test sites zoomed in at the right-hand side.

relatively cloud-free SPOT-6 image available was acquired on September 29th, 2016. Half of the samples were kept out of classification process (out-of-the-bag), to be used on the accuracy assessment (Bylander, 2002).

Table 3. Neural Network Classification Parameters

| Parameters | Value |
|---|---|
| Activation | Logistic |
| Training Threshold Contribution | 0.9 |
| Training Rate | 0.2 |
| Training Momentum | 0.9 |
| Training RMS Exit Criteria | 0.005 |
| Number of Hidden Layers | 1 |
| Number of Training Iterations | 50000 |

## 3. Result and Discussion

The geometric correction performed with the RMSE for each corresponding bands were kept kept at minimum (< 0.5 pixels). Figure 2 elaborate our approach to geometric correction and how it was able to rectify the blurriness. Figure 2a shows how distinct object such as cloud and waterbody did not have sharp edges due to the misalignment between LAPAN-A3 bands. After the geometric correction (figure 2b) these object appeared to have better and clearer edges

After geometrically corrected, LAPAN-A3 data were resampled to 30-meter pixel size. Both datasets were classified using MLC and ANN, and the results are as follow. In both AOI_1 and AOI_2, only 4 LULC classess were succesfully extracted. Meanwhile, ini AOI_3 there were 9 classes. The classification results for these classes are shown in figure 3 and figure 4 for MLC and ANN classifier, respectively. These figures act as a means of visual inspection to see the esthetic of generated LULC maps, as well as, elaborating the spatial distribution of each LULC classes extracted. For ANN classification on

LA3, the training period on all three AOI did not meet the maximum number of iteration set initially. It was only at 150, 700, and 700 iterations for AOI_1, AOI_2, and AOI_3 respectively. The main reason was because the RMS exit criteria had all met by the classifier.

Table 4 summarized the overall accuracy and κ value for both datasets. While Landsat-8 generally outperformed LAPAN-A3, it is encouraging to see that in some particular cases, LAPAN-A3 were able to outperform Landsat-8 in terms of OA. The OA on LAPAN-A3 at AOI_2 and AOI_3 was slightly higher than Landsat-8. Albeit the difference was not as high as 4 other cases, this results showcased a glimpse of LAPAN-A3 potential on extracting LULC information. Looking at figure 5, LAPAN-A3 overall accuracy pattern for all AOI resembles the same pattern of Landsat-8. Highest OA in AOI_1 followed by AOI_3, with AOI_2 was the least of them all. Looking specifically at AOI_3, which consists of almost twice as much classes as the other two AOIs, LAPAN-A3 performed relatively consistent, indicated by the highest kappa value of all three AOI. The OA difference between two classification algorithms in AOI_3 was only at 1.31%.

Bear in mind that each data set had not undergone any atmospheric correction, thus resulting in inherently different radiometric resolution. There are several solution that can be done to bridge this gap. Jensen (2005) suggest to decompress lower radiometric resolution data from 12bit to 16bit. The decompressed values, however, will not better that of the original. Looking at how Landsat-8 were outperformed LAPAN-A3 even with lower radiometric resolution, we decided to not pursue this method. The other solution offered by Jensen (2005) is to simply atmospherically corrected both dataset to gain the surface reflectance value. This option are also out of the question, since the proper parameters of LAPAN-A3 required on performing such correction have not been acquired.

Several studies have been conducted to see the effect of radiometric resolution on classification accuracy. Rao et al. (2007) found an incremental increase of 3% on higher radiometric data. Similar findings were
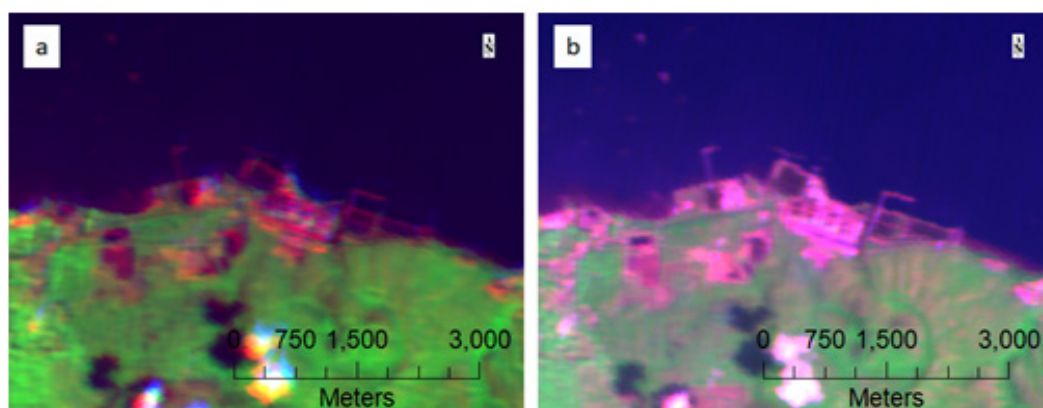


Figure 2. LAPAN-A3 RGB (Red-NIR-Green), (a) before geometric correction, and (b) After geometric correction
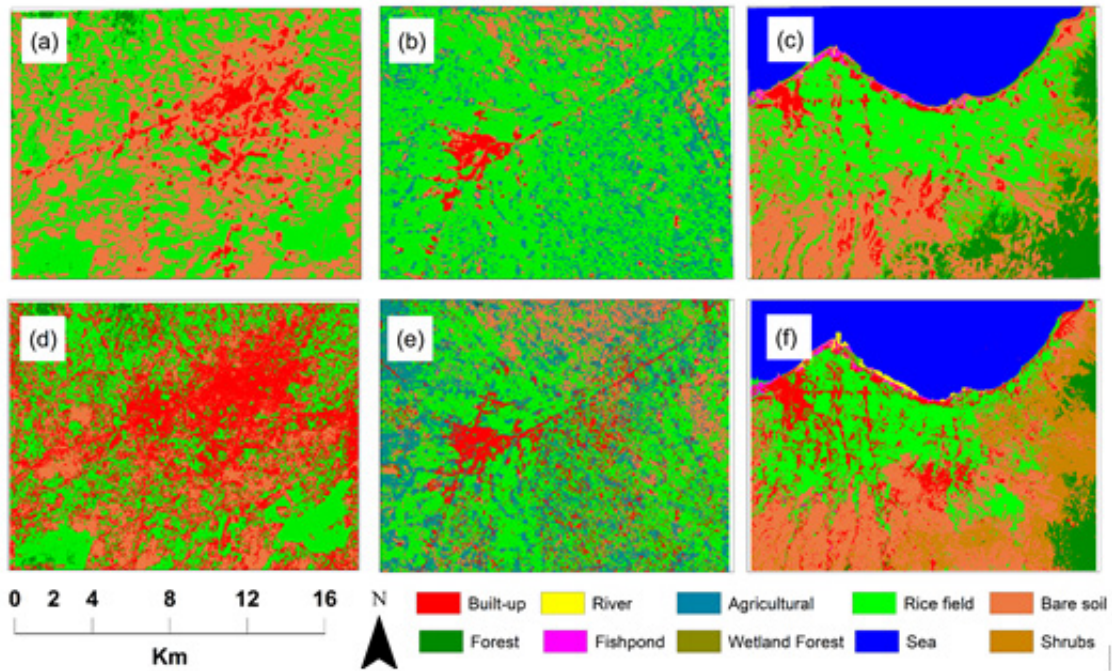
Figure 3. Output maps of classifications using MLC, (a) LAPAN-A3 AOI_1, (b) LAPAN-A3 AOI_2, (c) LAPAN-A3 AOI_3, (d) Landsat-8 AOI_1, (e) Landsat-8 AOI_2, (f) Landsat-8 AOI_3
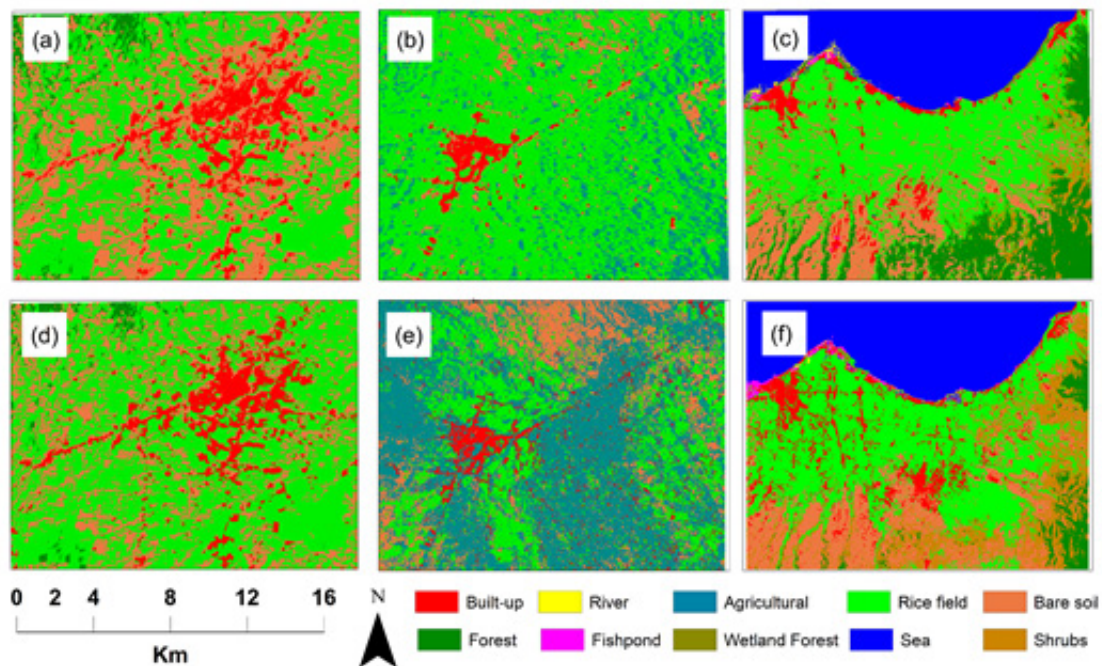


Figure 4. Output maps of classifications using ANN, (a) LAPAN-A3 AOI_1, (b) LAPAN-A3 AOI_2, (c) LAPAN-A3 AOI_3, (d) Landsat-8 AOI_1, (e) Landsat-8 AOI_2, (f) Landsat-8 AOI_3

also found by Verde et al. (2018), where the higher radiometric resolution data does not necessarily imply improved classification accuracy. Granted that Verde et al. (2018) were also found an 8% increase on classification accuracy using higher radiometric resolution, but then further explained how the use of spectral indices, texture information, and object-based classification render the higher radiometric only produced 1% increase. Franks & Masek (2007) were also found a small difference on

determining the forested environment by increasing the radiometric resolution above 8 bits. These previous studies are all implying that, despite the fact that higher radiometric resolution brings more depth to spectral information within an image, other factors such as spatial resolution, spectral resolution, classification frame work (pixel-based/object-based) plays more important role on classification accuracy. This then encourage us on further explaining our results.

Table 4. Overall Classification Accuracy,
κ values for two difference algorithm over three AOIs

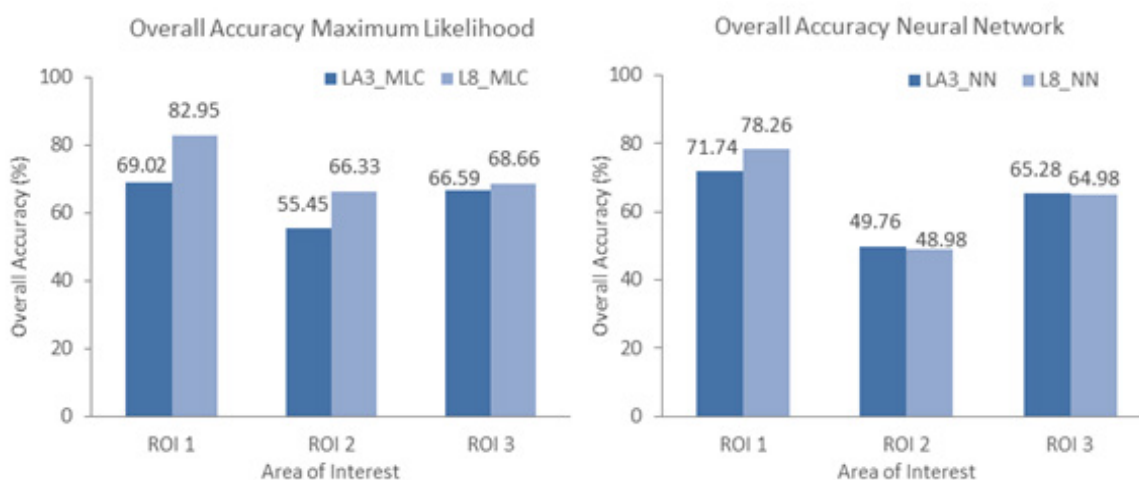| Classification Algorithm | AOI | Overall Accuracy | | κ value | |
|---|---|---|---|---|---|
| | | LAPAN-A3 Landsat-8 | Landsat-8 | LAPAN-A3 | Landsat-8 |
| MLC | 1 | 69.02% | 82.95% | 0.58 | 0.76 |
| | 2 | 55.45% | 66.33% | 0.41 | 0.55 |
| | 3 | 66.59% | 68.66% | 0.62 | 0.65 |
| ANN | 1 | 71.74% | 78.26% | 0.61 | 0.70 |
| | 2 | 49.76% | 48.98% | 0.33 | 0.32 |
| | 3 | 65.28% | 64.98% | 0.61 | 0.61 |



Figure 5. Overall accuracy for both datasets over three different test sites using (a) MLC, and (b) ANN
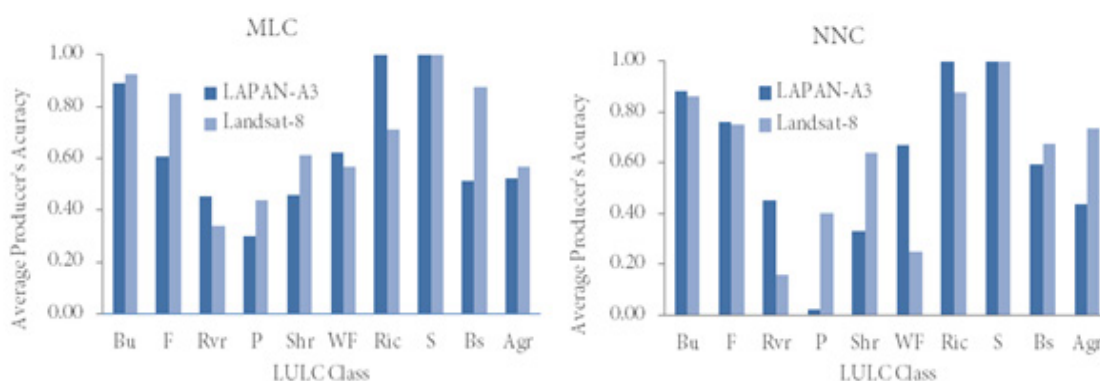


Figure 6. Average producer's accuracy over three AOI for both datasets using (a) MLC, and (b) ANN

Table 5 and Table 6 shows the error matrix for LAPAN-A3 using MLC and ANN algorithm respectively. Figure 6 summarized the producer's accuracy for all three AOI in both dataset. Looking at individual LULC classes, built-up, ricefield and sea, produced consistently acceptable accuracy for both classifers (Figure 6). These results seem to be consistent with other research that was conducted by Setiawan et al. (2018), who found that LAPAN-A3 Red and NIR band provide an adequate spectral discrimination of crop types in agricultural land. In accordance with the sea class, the previous study conducted by Nugroho et al. (2018) have demonstrated how well LAPAN-A3 were able to extract water body. It is also encouraging to know that built-up area can successfully extract by LAPAN-A3 with average producer's accuracy reaching 89% and 88% for MLC and ANN classifier, respectively. Forest classes often confused with Agricultural

Table 5. Error matrices of MLC over three AOI for LAPAN-A3

| (a) MLC AOI_1 | | Reference | | | | | |
|---|---|---|---|---|---|---|---|
| | | Bu | Agr | Bs | F | Total | UA |
| Classification | Bu | 46 | 0 | 0 | 0 | 46 | 1.00 |
| | Agr | 0 | 34 | 16 | 16 | 66 | 0.52 |
| | Bs | 6 | 19 | 33 | 0 | 58 | 0.57 |
| | F | 0 | 0 | 0 | 14 | 14 | 1.00 |
| | Total | 52 | 53 | 49 | 30 | 184 | |
| PA | | 0.88 | 0.64 | 0.67 | 0.47 | | |
| Average | PA = | 66.66% | UA = | 77.10% | OA = | 69.02% | |

| (b) MLC AOI_2 | | Reference | | | | | |
|---|---|---|---|---|---|---|---|
| | | Bu | Bs | R | Agr | Total | UA |
| Classification | Bu | 52 | 0 | 4 | 0 | 56 | 0.93 |
| | Bs | 5 | 11 | 0 | 10 | 26 | 0.42 |
| | R | 0 | 40 | 32 | 22 | 94 | 0.34 |
| | Agr | 0 | 0 | 13 | 22 | 35 | 0.63 |
| | Total | 57 | 51 | 49 | 54 | 211 | |
| PA | | 0.91 | 0.22 | 0.65 | 0.41 | | |
| Average | PA = | 54.71% | UA = | 58.02% | OA = | 55.45% | |

| (c) MLC AOI_3 | | Reference | | | | | | | | | | |
|---|---|---|---|---|---|---|---|---|---|---|---|---|
| | | Bu | F | Rvr | P | Sr | WF | Ric | S | Bs | Total | UA |
| Classification | Bu | 51 | 0 | 6 | 12 | 0 | 0 | 0 | 0 | 18 | 87 | 0.59 |
| | F | 0 | 32 | 0 | 0 | 11 | 0 | 0 | 0 | 0 | 43 | 0.74 |
| | Rvr | 0 | 0 | 13 | 0 | 0 | 0 | 0 | 0 | 0 | 13 | 1.00 |
| | P | 1 | 0 | 6 | 16 | 0 | 1 | 0 | 0 | 0 | 24 | 0.67 |
| | Shr | 0 | 3 | 0 | 0 | 24 | 0 | 0 | 0 | 0 | 27 | 0.89 |
| | WF | 0 | 0 | 2 | 2 | 0 | 36 | 0 | 0 | 0 | 40 | 0.90 |
| | Ric | 0 | 0 | 10 | 15 | 11 | 13 | 51 | 0 | 0 | 100 | 0.51 |
| | S | 0 | 0 | 1 | 0 | 0 | 0 | 0 | 48 | 0 | 49 | 0.98 |
| | Bs | 6 | 0 | 12 | 9 | 6 | 8 | 0 | 0 | 34 | 75 | 0.45 |
| | Total | 58 | 35 | 50 | 54 | 52 | 58 | 51 | 48 | 52 | 458 | |
| PA | | 0.88 | 0.74 | 0.26 | 0.30 | 0.46 | 0.62 | 1.00 | 1.00 | 0.65 | | |
| Average | PA = | 65.73% | UA = | 74.77% | OA = | 66.59% | | | | | |

Bu: Built-up, F: Forest, R: River, P: Fishpond, Sr: Shrubs, WF: Wetland Forest, Ric: Rice fields, S: Sea, Br: Bare soil, Agr: Agricultural land other than rice ML: Maximum Likelihood, AOI: Area of Interest, PA: Producer's Accuracy. UA: User's Accuracy, OA: Overall Accuracy

and/or Shrub classes, resulting in fairly moderate accuracy of 0.61 for two AOI using MLC. Using ANN, however, the average PA for forest increased to 0.76, which is slightly higher than Landsat-8 with 0.75.

The poorest accuracy were found on fishpond class. With the PA only reached 0.3 using MLC, and even lower 0.02 using ANN. It was often confused with baresoil, built-up, and ricefield classes. The possible explanation for this, that at the acquisition time, the fishpond were drained, thus giving similar reflectance to baresoil and built-up class. The shape of the fishpond as well as the existence of dikes surrounding them are making it similar to the ricefield, especially at the early stages of flooding and transplanting phase. This cunfusion worsened by the excessive mixel pixel that occurred on LAPAN-A3. This condition is apparent on Figure 3 and Figure 4, where the Landsat-8 results appeared to be sharper than LAPAN-A3, despite having lower spatial resolution.

While the geometric correction process managed to minimize the band-to-band misalignment, LAPAN-A3 still suffers from blurring effect. Inspecting each individual bands compared to Landsat-8 shows how these individual bands blurred in different ways. Figure 7 elaborates this blurring effect even more. To have a better view on this issue, we created a transect line over a man-made object with very distinct border. The transect

Table 6. Error matrices of ANN over three AOI for LAPAN-A3

| (a) MLC AOI_1 | | Reference | | | | | |
|---|---|---|---|---|---|---|---|
| | | Bu | Agr | Bs | F | Total | UA |
| Classification | Bu | 46 | 0 | 1 | 0 | 47 | 0.98 |
| | Agr | 0 | 36 | 17 | 11 | 64 | 0.56 |
| | Bs | 6 | 17 | 31 | 0 | 54 | 0.57 |
| | F | 0 | 0 | 0 | 19 | 19 | 1.00 |
| | Total | 52 | 53 | 49 | 30 | 184 | |
| PA | | 0.88 | 0.68 | 0.63 | 0.63 | | |
| Average | PA = | 70.75% | UA = | 77.88% | OA = | 71.74% | |

| (b) MLC AOI_2 | | Reference | | | | | |
|---|---|---|---|---|---|---|---|
| | | Bu | Bs | R | Agr | Total | UA |
| Classification | Bu | 48 | 0 | 4 | 0 | 52 | 0.92 |
| | Bs | 7 | 15 | 0 | 5 | 27 | 0.56 |
| | R | 2 | 36 | 32 | 39 | 109 | 0.29 |
| | Agr | 0 | 0 | 13 | 10 | 23 | 0.43 |
| | Total | 57 | 51 | 49 | 54 | 211 | |
| PA | PA | 0.84 | 0.29 | 0.65 | 0.19 | | |
| Average | PA = | 49.36% | UA = | 55.17% | OA = | 49.76% | |

| (c) MLC AOI_3 | | Reference | | | | | | | | | | |
|---|---|---|---|---|---|---|---|---|---|---|---|---|
| | | Bu | F | Rvr | P | Sr | WF | Ric | S | Bs | Total | UA |
| Classification | Bu | 54 | 0 | 6 | 26 | 0 | 0 | 0 | 0 | 7 | 93 | 0.58 |
| | F | 0 | 31 | 8 | 8 | 15 | 11 | 0 | 0 | 0 | 73 | 0.42 |
| | Rvr | 0 | 0 | 13 | 1 | 0 | 0 | 0 | 0 | 0 | 14 | 0.93 |
| | P | 0 | 0 | 8 | 1 | 0 | 0 | 0 | 0 | 0 | 9 | 0.11 |
| | Shr | 0 | 4 | 0 | 0 | 17 | 0 | 0 | 0 | 0 | 21 | 0.81 |
| | WF | 0 | 0 | 3 | 1 | 0 | 39 | 0 | 0 | 0 | 43 | 0.91 |
| | Ric | 0 | 0 | 11 | 15 | 19 | 5 | 51 | 0 | 0 | 101 | 0.50 |
| | S | 0 | 0 | 0 | 2 | 0 | 3 | 0 | 48 | 0 | 53 | 0.91 |
| | Bs | 4 | 0 | 1 | 0 | 1 | 0 | 0 | 0 | 45 | 51 | 0.88 |
| | Total | 58 | 35 | 50 | 54 | 52 | 58 | 51 | 48 | 52 | 458 | |
| PA | | 0.93 | 0.89 | 0.26 | 0.02 | 0.33 | 0.67 | 1.00 | 1.00 | 0.87 | | |
| Average | PA = | 66.22% | UA = | 67.27% | OA = | 65.28% | | | | | |

Bu: Built-up, F: Forest, R: River, P: Fishpond, Sr: Shrubs, WF: Wetland Forest, R: Rice fields, S: Sea, Br: Bare soil, Agr: Agricultural land other than rice ML: Maximum Likelihood, AOI: Area of Interest, PA: Producer's Accuracy. UA: User's Accuracy, OA: Overall Accuracy

line spanned 22 pixels (± 630m) from west to east. In order to bridge the gap between DN due to difference radiometric quantifications, both dataset's DN were normalized. The normalized DN ranged from 0-1.

Figure 7a shows the location of a subset data that we used. To look closer on the area, figure 7b shows the same area using SPOT-6 Pan-sharpened data (1.5 m). The transect line went over a rice field and a patch of a bright building. Figure 7e shows how the DN over the transect line form a steep cliff in Landsat-8 data with a distinct peak for all three bands on the bright object to the west (figure 7c). LAPAN-A3, on the other hand, gave a plateau-like profile on the same object,

which spanned from 4 to 6 pixels. The blurring effect even creates another peak on LAPAN-A3 for Blue and green band, corresponding to a slightly smaller building on the west (figure 7d). This indicates that the blurring effect on LAPAN-A3 occurs for both across and along-track of the satellite. Pre-flight measurement conducted by Tahir et al. (2016) revealed that the blurring effect caused by the difference in each channel detector inside the CCD sensor of LISA. This then contributed the difference in each bands image focus quality, thus created the unnecessary mixed pixel. This paper agrees to previous studies on acknowledging mixed pixel as a major problem
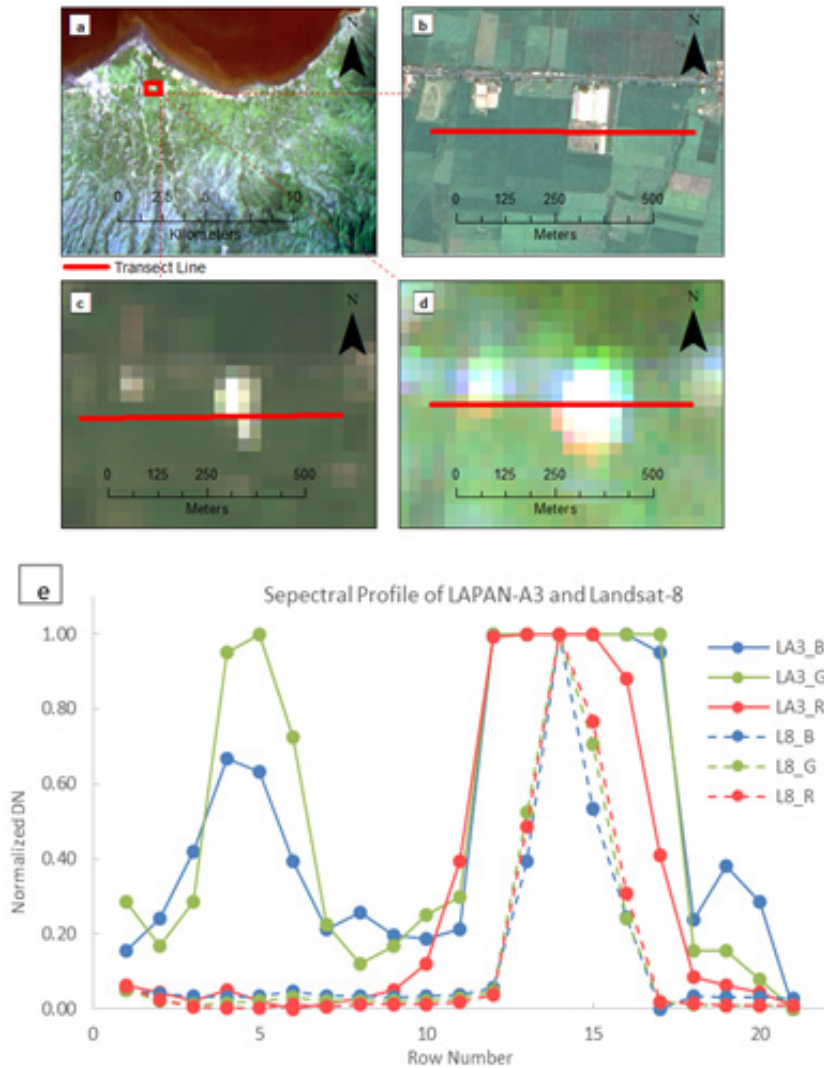
Figure 7. Blurring effect on LAPAN-A3 data compared to Landsat-8, (a) emphasized on a subset of AOI_3, (b) Natural color RGB Composite of SPOT-6 Pansharpened, (c) RGB 321 of LAPAN-A3, (d) RGB 432 of Landsat-8 OLI, (e) Spectral profile over the transect line for two datasets with 3 visible bands. Dashed and continous lines correspond to Landsat-8 and LAPAN-A3 bands respectively.

on medium resolution EO data, affecting the pixel-based classifier (Cracknell, 1998; Weng, 2012), but the addition of blurriness should take into consideration when extracting the LULC information. Blurring effect on CCD sensor's imagery was also found on other platforms. Namely CBERS-1 (K. Bensebaa, Banon, & Fonseca, 2012) and CBERS-2 (Kamel Bensebaa, Banon, Fonseca, & Erthal, 2008; Junior & Tommaselli, 2013). A validation and calibration process of KOMPSAT-2 imagery done by Lee et al. (2011) also briefly discussed this blurring effect and how to compensate for it. To get the more comprehensive understanding on LAPAN-A3 blurriness, a further quantitative analysis should be done, referring to the aforementioned study. This, unfortunately, is outside of this paper's scope.

Figure 7. Blurring effect on LAPAN-A3 data compared to Landsat-8, (a) emphasized on a subset of AOI_3, (b) Natural color RGB Composite of SPOT-6 Pansharpened, (c) RGB 321 of LAPAN-A3, (d) RGB 432 of Landsat-8 OLI, (e) Spectral profile over the transect line for two datasets with 3 visible bands. Dashed and continous lines correspond to Landsat-8 and LAPAN-A3 bands respectively.

An arguable weakness of this study was the used of the same sample quantity for both classifiers. This study used samples designated to perform ML classification, while machine learning algorithm such as ANN would thrive with smaller training sample compared to conventional MLC (G. Foody, McCulloch, & Yates, 1995; Hepner, Logan, Pitter, & Bryant, 1990). Thus, the maximum potential of using ANN to derive LULC from LAPAN-A3 has no fully explored. Numerous study have been conducted to maximize ANN. Namely, the use of texture information

(Bischof, Pinz, & Schneiden, 1992; Gandhi, 2004), or the optimized parameter guidelines suggested by Kavzoglu & Mather (2003). Further investigation on optimizing LULC extraction is strongly recommended.

## 4.Conclusion

This study shows moderate mapping ability from LAPAN-A3 using two different classification algorithm, with overall accuracy reaching 71% at one test site. Compared to Landsat-8, the overall accuracy of LAPAN-A3 are generally lower. It is, however, exibit a similar pattern in term of OA's variability over three different test sites. The OA's difference between LAPAN-A3 and Landsat-8 varies between 2% - 15%. From individual LULC classes point of view, only a few of these classes was successfully extracted with sufficient accuracy. Built-up, forest, Sea, and ricefield are the top 4 LULC classes that were succesfully extracted. With the abundant methodology yet to be explored with LAPAN-A3 data, we believed that the findings in this study deserves to be followed up. Time series analysis of LAPAN-A3 data can be useful for monitoring large water body. Keeping in mind that the analysis was done using DN with no prior radiometric correction, it is encouraging to know that there is still rooms for improvements, provided that the existing issued on LAPAN-A3 imagery addressed and corrected.

## Acknowledgment

## References

Bailly, J. S., Arnaud, M., & Puech, C. (2007). Boosting: a classification method for remote sensing. International Journal of Remote Sensing, 28(7), 1687–1710. https://doi.org/10.1080/01431160500469985

Bensebaa, K., Banon, G. J. F., & Fonseca, L. M. G. (2012). Spatial resolution estimation of CBERS-1 and CBERS-2 CCD cameras. International Journal of Remote Sensing, 33(2), 604–629. https://doi.org/10.1080/01431161.2010.545840

Bensebaa, K., Banon, G. J. F., Fonseca, L. M. G., & Erthal, G. J. (2008). On-orbit Spatial Resolution Estimation of CBERS-2 Imaging System Using Ideal Edge Target. In E. Damiani, K. Yétongnon, P. Schelkens, A. Dipanda, L. Legrand, & R. Chbeir (Eds.), Signal Processing for Image Enhancement and Multimedia Processing (pp. 37–48). Boston, MA: Springer US. https://doi.org/10.1007/978-0-387-72500-0_4

Bischof, H., Pinz, A. J., & Schneiden, W. (1992). Multispectral Classification of Landsat-Images

Using Neural Networks. IEEE Transactions on Geoscience and Remote Sensing, 30(3), 482–490. https://doi.org/10.1109/36.142926

BSN. (2014). Klasifikasi penutup lahan - Bagian 1 : Skala kecil dan menengah. Badan Standarisasi Nasional.

Bylander, T. (2002). Estimating generalization error on two-class datasets using out-of-bag estimates. Machine Learning, 48(1–3), 287–297. https://doi.org/10.1023/A:1013964023376

Cohen, J. (1960). A coefficient of agreement for nominal scales. Educational and Psychological Measrurement, XX(1), 37–46.

Congalton, R. G., & Green, K. (2009). Assessing the Accuracy of Remotely Sensed Data: Principles and Practices. CRC Press/Taylor & Francis.

Cracknell, a P. (1998). Synergy in remote sensing - what' s in a pixel ? International Journal of Remote Sensing, 19(11), 2025–2047. https://doi.org/10.1080/014311698214848

Dai, X. (1998). The effects of image misregistration on the accuracy of remotely sensed change detection. IEEE Transactions on Geoscience and Remote Sensing, 36(5 PART 1), 1566–1577. https://doi.org/10.1109/36.718860

Danoedoro, P. (2012). Pengantar Penginderaan Jauh Digital (I). Yogyakarta: Penerbit ANDI.

Du, Y., Zhang, Y., Ling, F., Wang, Q., Li, W., & Li, X. (2016). Water bodies' mapping from Sentinel-2 imagery with Modified Normalized Difference Water Index at 10-m spatial resolution produced by sharpening the swir band. Remote Sensing, 8(4). https://doi.org/10.3390/rs8040354

Foody, G. M., & Arora, M. K. (1997). An evaluation of some factors affecting the accuracy of classification by an artificial neural network. International Journal of Remote Sensing, 18(4), 799–810. https://doi.org/10.1080/014311697218764

Foody, G., McCulloch, M., & Yates, W. (1995). Classification of remotely sensed data by an artificial neural network: issues related to training data characteristics. Photogrammetric Engineering & Remote Sensing, 61(4), 391–401. Retrieved from http://cat.inist.fr/?aModele=afficheN&cpsidt=3496683

Franks, S., & Masek, J. G. (2007). How many bits? Radiometric Resolution as a Factor in Obtaining Forestry Information with Remotely Sensed Measurements. In IEEE International Geoscience and Remote Sensing Symposium (pp. 1291–1294).

Gandhi, V. (2004). Image Classification Based on Textural Features using Artificial Neural Network ( ANN ). Journal of The Institution of Engineers (India), 84, 72–77.

Hakim, P. R., Hasbi, W., & Syafrudin, A. H. (2014). ADCS requirements of Lapan-A3 satellite based on image geometry analysis. Proceeding - ICARES 2014: 2014 IEEE International Conference on Aerospace Electronics and

Remote Sensing Technology, 142–146. https://doi.org/10.1109/ICARES.2014.7024383

Hakim, P. R., & Permala, R. (2017). Analysis of LAPAN-IPB image lossless compression using differential pulse code modulation and huffman coding. In IOP Conference Series: Earth and Environmental Science (Vol. 54, p. 012096). IOP Publishing. https://doi.org/10.1088/1755-1315/54/1/012096

Hakim, P. R., Syafrudin, A. H., & Utama, S. (2017). Band Co-registration Distortion Modeling of LAPAN-A3 Multispectral Imager Based on Satellite Attitude. The 4th International Symposium on LISAT 2017. Bogor, Indonesia.

Han, N., Wu, J., Tahmassebi, A. R. S., Xu, H. W., & Wang, K. (2011). NDVI-based lacunarity texture for improving identification of torreya using object-oriented method. Agricultural Sciences in China, 10(9), 1431–1444. https://doi.org/10.1016/S1671-2927(11)60136-3

Hasbi, W., & Suhermanto. (2013). Development of LAPAN-A3 / IPB Satellite an Experimental Remote Sensing Microsatellite. In 34th Asian Conference on Remote Sensing 2013, ACRS 2013 (p. 8). Bali. Retrieved from http://a-a-r-s.org/acrs/index.php/acrs/acrs-overview/proceedings-1?view=publication&task=show&id=1365

Hepner, G. F., Logan, T., Pitter, N., & Bryant, N. (1990). Artificial Neural Network Classification Using a Minimal Training Set : Comparison to Conventional Supervised Classification. Photogrammetric Engineering & Remote Sensing, 56(4), 469–473.

Jensen, J. R. (2005). Introductory Digital Image Processing: A Remote Sensing Perspective (3rd Ed.). Pearson Education.

Junior, J. M., & Tommaselli, A. M. G. (2013). Exterior orientation of CBERS-2B imagery using multi-feature control and orbital data. ISPRS Journal of Photogrammetry and Remote Sensing, 79, 219–225. https://doi.org/10.1016/j.isprsjprs.2013.02.018

Kanellopoulos, I., Wilkinson, G. G., & Megier, J. (1993). Integration of neural network and statistical image classification for land cover mapping. In Proceedings of IGARSS '93 - IEEE International Geoscience and Remote Sensing Symposium (pp. 511–513). Tokyo, Japan: IEEE. https://doi.org/10.1109/IGARSS.1993.322597

Kavzoglu, T., & Mather, P. M. (2003). The use of backpropagating artificial neural networks in land cover classification. International Journal of Remote Sensing, 24(23), 4907–4938. https://doi.org/10.1080/0143116031000114851

Knipling, E. B. (1970). Physical and Physiological Basis for the Reflectance of Visible and Near Infrared Radiation from Vegetation. Remote Sensing of Environment, 1, 155–159.

Kushardono, D., Fukue, K., & Shimoda, H. (1995). Optimized Neural Network for Spatial Land cover with the aid of Co-occurrence Matrix. Journal of the Japan Society of Photogrammetry and Remote Sensing, 34(4), 22–35. https://doi.org/10.4287/jsprs.34.4_22

Lee, D. H., Yang, J. Y., Seo, D. C., Song, J. H., Chung, J. H., & Lim, H. S. (2011). Image restoration of the asymmetric point spread function of a high-resolution remote sensing satellite with time-delayed integration. Advances in Space Research, 47(4), 690–701. https://doi.org/DOI 10.1016/j.asr.2010.10.006

Li, G., Li, X., Li, G., Wen, W., Wang, H., Chen, L., … Deng, F. (2013). Comparison of spectral characteristics between China HJ1-CCD and landsat 5 TM imagery. IEEE Journal of Selected Topics in Applied Earth Observations and Remote Sensing, 6(1), 139–148. https://doi.org/10.1109/JSTARS.2012.2206800

Liu, X. H., Skidmore, A. K., & Van Oosten, H. (2002). Integration of classification methods for improvement of land-cover map accuracy. ISPRS Journal of Photogrammetry and Remote Sensing, 56(4), 257–268. https://doi.org/10.1016/S0924-2716(02)00061-8

McFeeters, S. K. (1996). The use of the Normalized Difference Water Index (NDWI) in the delineation of open water features. International Journal of Remote Sensing, 17(7), 1425–1432. https://doi.org/10.1080/01431169608948714

Nugroho, J. T., Zylshal, Z., & Kushardono, D. (2018). LAPAN-A3 Satellite Data Analysis for Land Cover Classificationb (Case Study: Toba Lake Area, North Sumatra). International Journal of Remote Sensing and Earth Sciences, 15(1), 71–80. https://doi.org/10.30536/j.ijreses.2018.v15.a2782

Parker, J. a, Kenyon, R. V, & Troxel, D. E. (1983). Comparison of interpolation methods for image resampling. IEEE Transactions on Medical Imaging, 2(1), 31–39. https://doi.org/10.1109/42.7784

PUSTEKSAT. (2016). Spesisikasi Teknis Satelit LAPAN-A3. Retrieved January 16, 2017, from http://pusteksat.lapan.go.id/index.php/subblog/pages/2014/39/Spesisikasi-Teknis-Satelit-LAPAN-A3

Rao, N. R., Garg, P. K., & Ghosh, S. K. (2007). Evaluation of radiometric resolution on land use/land cover mapping in an agricultural area. International Journal of Remote Sensing, 28(2), 443–450. https://doi.org/10.1080/01431160600733181

Richards, J. A. (1993). Remote Sensing Digital Image Analysis. Berlin/Heidelberg: Springer-Verlag. https://doi.org/10.1007/3-540-29711-1

Rumelhart, D. E., Hinton, G. E., & Williams, R. J. (1986). Learining Internal Representations by Error Propagation. In Parallel Distributed Processing: Explorations in the Microstructure of Cognition (Vol. 1, pp. 318–362). MIT Press. https://doi.org/10.1016/B978-1-4832-1446-7.50035-2

Schowengerdt, R. A. (1983). Techniques for image processing and classification in remote sensing. Academic Press. Retrieved from http://www.

sciencedirect.com/science/book/9780126289800

Setiawan, Y., Prasetyo, L. B., Pawitan, H., Liyantono, L., Syartinilia, S., Wijayanto, A. K., … Hakim, P. R. (2018a). Pemanfaatan Fusi Data Satelit Lapan-a3/Ipb Dan Landsat 8 Untuk Monitoring Lahan Sawah. Jurnal Pengelolaan Sumberdaya Alam Dan Lingkungan (Journal of Natural Resources and Environmental Management), 8(1), 67–76. https://doi.org/10.29244/jpsl.8.1.67-76

Setiawan, Y., Prasetyo, L. B., Pawitan, H., Liyantono, L., Syartinilia, S., Wijayanto, A. K., … Hakim, P. R. (2018b). Pemanfaatan Fusi Data Satelit Lapan-a3/Ipb Dan Landsat 8 Untuk Monitoring Lahan Sawah. Jurnal Pengelolaan Sumberdaya Alam Dan Lingkungan (Journal of Natural Resources and Environmental Management), 8(1), 67–76. https://doi.org/10.29244/jpsl.8.1.67-76

Tahir, A. M., Hakim, P. R., Syafruddin, A. H., Cagak, J., Km, S., & Indonesia, B. (2016). Image-Focusing Quality Improvement on Lapan-A3 Satellite Multispectral Imager. Jurnal Teknologi Dirgantara, 14(1), 37–50. Retrieved from http://www.jurnal.lapan. go.id/index.php/jurnal_tekgan/article/view/2566

Tucker, C. J., & Sellers, P. J. (1986). Satellite remote sensing of primary production. International Journal of Remote Sensing, 7(11), 1395–1416. https://doi.org/10.1080/01431168608948944

USGS. (2012). Landsat Data Continuity Mission ( Ldcm ) Mission Data Data Format Control Book ( Dfcb ), (October).

Veraverbeke, S., Gitas, I., Katagis, T., Polychronaki, A., Somers, B., & Goossens, R. (2012). Assessing post-fire vegetation recovery using red-near infrared vegetation indices: Accounting for background and vegetation variability. ISPRS Journal of Photogrammetry and Remote Sensing, 68(1), 28–

39. https://doi.org/10.1016/j.isprsjprs.2011.12.007

Verde, N., Mallinis, G., Tsakiri-Strati, M., Georgiadis, C., & Patias, P. (2018). Assessment of radiometric resolution impact on remote sensing data classification accuracy. Remote Sensing, 10(8), 1–17. https://doi.org/10.3390/rs10081267

Wahid, D. A., & Akiyama, T. (2007). Possibilities of landuse / landcover classification using ALOS AVNIR-2 in Takayama. Journal of the Japan Society of Photogrammetry and Remote Sensing, 46(5), 56–67. https://doi.org/http://doi.org/10.4287/jsprs.46.5_56

Weng, Q. (2012). Remote sensing of impervious surfaces in the urban areas: Requirements, methods, and trends. Remote Sensing of Environment, 117, 34–49. https://doi.org/10.1016/j.rse.2011.02.030

Yoshioka, H., Huete, A. R., & Miura, T. (2000). Derivation of vegetation isoline equations in red-NIR reflectance space. IEEE Transactions on Geoscience and Remote Sensing, 38(2 I), 838–848. https://doi.org/10.1109/36.842012

Zylshal, Z., Sari, N. M., Nugroho, J. T., & Kushardono, D. (2017). Comparison of Spectral Characteristic between LAPAN-A3 and Sentinel-2A. IOP Conference Series: Earth and Environmental Science, 98(1), 012051. https://doi.org/10.1088/1755-1315/98/1/012051